Eur. Phys. J. B (2013) 86: 138
DOI: 10.1140/epjb/e2013-30917-6

THE EUROPEAN PHYSICAL JOURNAL B

Regular Article

# Macroscopic quantum beats in a molecular magnet loosely fastened to the matrix

Gwang-Hee Kim[a]

Department of Physics, Sejong University, 143747 Seoul, Republic of Korea

Received 10 October 2012 / Received in final form 20 December 2012
Published online 8 April 2013 – 

**Abstract.** It is shown that, in the presence of sound waves, rotational states play an important role in the spin oscillation of a free nanomagnet. Employing the rotating wave approximation and perturbation theory, we compute the magnetization dynamics generated by ultrasound and discuss optimal conditions under which this novel quantum effect can be observed in a rotating single-molecule magnet.

## 1 Introduction

Investigations of macroscopic quantum tunneling in nanospin systems have been a topical issue of intensive studies over the past few years [1–3]. Nanomagnets, called single-molecule magnets (SMM), have been such good candidates because all the clusters are mono-dispersed and the spin ground state and magnetic anisotropy are known with great accuracy. These molecules exhibit particularly interesting phenomena such as quantum tunneling of the magnetization [4–8], topological interference [9,10], and quantum coherence [11]. Such phenomena have received much attention, both theoretically and experimentally, in view of the macroscopic realization of quantum phenomena, and also because of some potential applications to molecular devices [12–19]. Many efforts have been made to understand their mechanisms by considering the Landau-Zener theory in SMMs. In those mechanisms, spin-phonon interactions have been recognized as playing an important role in the quantum dynamics of magnetization in SMMs [20].

Theoretical studies of the spin oscillation in nanospin systems have been around for some time. Among them, Calero and Chudnovsky [21] first raised the Rabi oscillation issue in the longitudinal anisotropy system with an external sound wave. Since then, Kim and Chudnovsky [22] and Kim [23] have studied the spin oscillation generated by an acoustic wave during the field sweep and suggested the observability of the spin oscillation in a macroscopic experiment. However, previous theoretical investigations of the spin oscillation have been discussed for a nanomagnetic system firmly fixed to a solid matrix so that their physical position and orientation were fixed and only rotation of the magnetization was allowed. In fact, partial or total decoupling of a system from the environment appears prevalent in nanomagnetic systems [12–19]. Very recently, the issue of the rotational states of a nanomagnet was studied by Chudnovsky and Garanin [24], who showed that the ground state of a nanomagnet that is free to rotate depends on several parameters such as the moment of inertia and total angular momentum of the system. Hence, it is of interest to study the spin oscillation generated by the sound wave in a SMM which is free to rotate, or loosely fastened to the substrate.

In this work, we demonstrate that the structure of a spin oscillation depends on the coupling constant of the system to the matrix, as well as the external parameters associated with the sound wave. The optimal condition for pronounced quantum beats is obtained by adjusting the frequency of the sound to the Rabi oscillation at a given value of total angular momentum. In this respect, the quantum beat of the magnetization is expected to be more diverse, due to the presence of such parameters, and measurable in molecular devices.

The rest of the article is organized as follows. In Section 2, introducing a pseudospin formulation, we obtain the effective Hamiltonian generated by the acoustic wave. In Section 3, we study the coupling of the spin system to the mechanical angular momentum in a free SMM and obtain the time evolution of its wave function. In Section 4, employing the rotating wave approximation and perturbation theory, we present the approximate form of the probability of finding the spin in the ground state and the expectation value of the $z$ projection of the spin. Detailed analysis shows that a quantum beat with a large period becomes more pronounced at two optimal conditions. A comparison of the results will be made with numerical ones. The conclusions are given in Section 5.

## 2 Two level system in the presence of sound waves

Consider the spin model described by the Hamiltonian

$$\mathcal{H}_{\rm SMM} = -DS_z^2 + \mathcal{H}_\perp, \tag{1}$$

where $S_i$ $(i = x, y, z)$ are three components of the spin operator, $D$ $(> 0)$ is the second order longitudinal anisotropy

[a] e-mail: gkim@sejong.ac.kr

constant and $\mathcal{H}_\perp$ is a small term that does not commute with $S_z$ and, thus, allows tunneling of $\mathbf{S}$ between states.

Applying an acoustic wave polarized along the $y$ axis and running along the $x$ axis, one obtains local rotation given by [25]

$$\delta\hat{\theta}(\mathbf{r}) = \frac{\omega}{2c_t} u_0 \cos(kx - \omega t)\hat{z}, \tag{2}$$

where $\omega(=c_t k)$, $k$, $u_0$ and $c_t$ are the frequency, wave vector, amplitude, and velocity of the transverse sound, respectively. Rotation by an angle $\delta\theta$ about the anisotropy axis, $Z$, transforms the spin Hamiltonian into the laboratory-frame Hamiltonian [21–23]

$$\mathcal{H} = e^{-i\delta\hat{\theta}\cdot\mathbf{S}} \mathcal{H}_{\rm SMM} e^{i\delta\hat{\theta}\cdot\mathbf{S}}. \tag{3}$$

In order to find the wave function in the laboratory frame, $|\Psi\rangle$, it is useful to introduce the lattice-frame wave function, $|\Psi^{(\rm lat)}\rangle$, which is related through

$$|\Psi^{(\rm lat)}\rangle = e^{i\delta\hat{\theta}\cdot\mathbf{S}} |\Psi\rangle. \tag{4}$$

Plugging it into the Schödinger equation, we obtain the lattice-frame Hamiltonian

$$\mathcal{H}^{(\rm lat)} = \mathcal{H}_{\rm SMM} - \hbar\mathbf{S}\cdot\mathbf{\Omega}, \tag{5}$$

where

$$\mathbf{\Omega}\left[\equiv \frac{\partial(\delta\hat{\theta})}{\partial t}\right] = \frac{\omega^2}{2c_t} u_0 \sin(kx - \omega t)\hat{z}. \tag{6}$$

We will solve the problem locally for each spin in the lattice frame and then make use of the above formula to obtain the solution for the entire system in the laboratory frame.

Without $\mathcal{H}_\perp$ and the sound wave, the unperturbed Hamiltonian has eigenvalues $E_m = -Dm^2$, where $\hat{S}_z|m\rangle = m|m\rangle$. In the absence of an external field along the $z$ axis, the lowest energy levels on both sides of the barrier are doubly degenerate, $E_{-S} = E_S$. The transverse operator $\mathcal{H}_\perp$ in the Hamiltonian (1) perturbs the $|\pm S\rangle$ and provides the level splitting ($\Delta$), which results in the avoided level crossing between two states $|-S\rangle$ and $|S\rangle$. Then, the ground state and the first excited state are even and odd combinations of $|\pm S\rangle$, respectively[1],

$$|\phi_\pm\rangle = \frac{1}{\sqrt{2}}\left(|S\rangle \pm |-S\rangle\right) \tag{7}$$

where $\Delta$ is the level splitting between the ground state $|\phi_+\rangle$ and the first excited state $|\phi_-\rangle$. Since the low energy spin states of SMM are superpositions of $|\pm S\rangle$, it makes sense to project the Hamiltonian on the $|\pm S\rangle$ states, making the system essentially a two-state system with a pseudospin of 1/2 whose components are

$$\begin{aligned}
\hat{\sigma}_x &= |-S\rangle\langle S| + |S\rangle\langle -S|,\\
\hat{\sigma}_y &= i|-S\rangle\langle S| - i|S\rangle\langle -S|,\\
\hat{\sigma}_z &= |S\rangle\langle S| - |-S\rangle\langle -S|.
\end{aligned} \tag{8}$$

Noting that $\mathcal{H}_{\rm SMM}|\phi_\pm\rangle = \mp\frac{\Delta}{2}|\phi_\pm\rangle$, the projection of the Hamiltonian (5) onto $|\pm S\rangle$ becomes the effective Hamiltonian [21]

$$\mathcal{H}^{(\rm lat)}_{\rm eff} = -\frac{\Delta}{2}\hat{\sigma}_x - \hbar S\Omega_z\hat{\sigma}_z, \tag{9}$$

where

$$\Omega_z = \frac{\omega_R}{S}\sin(kx - \omega t), \tag{10}$$

$$\omega_R = \frac{\omega^2}{2c_t} u_0 S. \tag{11}$$

## 3 Spin-rotation coupling

Now, we consider a SMM that is loosely fastened to the matrix in the presence of the acoustic wave. The effect of the local deformation of the SMM produced by the sound wave is contained in the Hamiltonian (5) with the local frequency $\mathbf{\Omega}(x,t)$. Hence, in order to study low-energy eigenstates of the SMM, we perform the transformation of the Hamiltonian (5) by employing the rotational operator [21,26]

$$\tilde{\mathcal{H}}^{(\rm lat)} = e^{-iS_z\phi}\mathcal{H}^{(\rm lat)}e^{iS_z\phi}. \tag{12}$$

Note that $\mathcal{H}^{(\rm lat)}$ includes the local ac field in equation (5).

Projecting the Hamiltonian (12) onto $|\pm S\rangle$, one obtains the generalization of equation (9):

$$\tilde{\mathcal{H}}^{(\rm lat)}_{\rm eff} = -\frac{\Delta}{4}\left[e^{-2iS\phi}\hat{\sigma}_+ + e^{2iS\phi}\hat{\sigma}_-\right] - \hbar S\Omega_z\hat{\sigma}_z, \tag{13}$$

where $\hat{\sigma}_\pm = \hat{\sigma}_x \pm i\hat{\sigma}_y$.

The full Hamiltonian of a SMM rotating around the $Z$ axis is expressed as

$$\begin{aligned}
\tilde{\mathcal{H}}^{(\rm lat)}_{{\rm eff},L} = &\frac{\hbar^2\hat{L}_z^2}{2I_z} - \hbar S\Omega_z\hat{\sigma}_z\\
&- \frac{\Delta}{4}\left[e^{-2iS\phi}\hat{\sigma}_+ + e^{2iS\phi}\hat{\sigma}_-\right],
\end{aligned} \tag{14}$$

where $\hat{L}_z = -i\partial_\phi$ is the operator of the mechanical angular momentum and $I_z$ is the moment of inertia of the SMM. We are now in a position to find the eigenstates of the rotating magnet. Noting that $[\tilde{\mathcal{H}}^{(\rm lat)}_{{\rm eff},l}, J_z] = 0$, where $J_z = L_z + S_z$, we need to use a basis that is a direct product of the two states basis for the spin and the mechanical basis for the rotational body. Before studying the time evolution of the wave function, we first need to find

[1] Actually, opeartor $\mathcal{H}_\perp$ slightly perturbs the $|\pm S\rangle$ states, adding to them small contribution of other $m_S$ states. However, even though we make use of $|\pm S\rangle$ instead of such degenerate normalized perturbed states, the conclusions are unchanged. Hence, in the ensuing discussion we will use $|\pm S\rangle$ for the degenerate normalized states.

**Table 1.** Critical value of $\gamma_J$ that separates $J-1$ and $J$ states of the molecular magnet with $S = 10$ and the corresponding value of $\chi$.

| $J$ | 1 | 2 | 3 | 4 | 5 |
|---|---|---|---|---|---|
| $\gamma_J$ | 1.0025 | 1.0127 | 1.0341 | 1.0689 | 1.1212 |
| $\chi$ | 0.10025 | 0.20254 | 0.31023 | 0.42754 | 0.56059 |
| $J$ | 6 | 7 | 8 | 9 | 10 |
| $\gamma_J$ | 1.1989 | 1.3176 | 1.5138 | 1.9007 | 3.2066 |
| $\chi$ | 0.71932 | 0.92229 | 1.211 | 1.7106 | 3.2066 |

the starting conditions, and thus write the eigenstates at $x = 0$ and $t = 0$ as [24]

$$\left|\Phi_J^{(0)}\right\rangle = \frac{1}{\sqrt{2}}(C_S|S\rangle \otimes |J-S\rangle_L + C_{-S}|-S\rangle \otimes |J+S\rangle_L), \quad (15)$$

where $J = m_J$ and the index $L$ indicates states in mechanical space with $\langle\phi|m_L\rangle = \exp(im_L\phi)/\sqrt{2\pi}$. The solution of $\tilde{\mathcal{H}}_{\mathrm{eff},L}^{(\mathrm{lat})}|\Phi_J^{(0)}\rangle = E_J|\Phi_J^{(0)}\rangle$ at $x = 0$ and $t = 0$ gives

$$E_{J\pm} = \frac{\Delta}{2}\left[\frac{1}{2\gamma}\left(\gamma^2+\chi^2\right) \pm \sqrt{1+\chi^2}\right], \quad (16)$$

and the corresponding coefficients given by

$$C_S^{(\pm)} = \sqrt{1 \pm \frac{\chi}{\sqrt{1+\chi^2}}},$$
$$C_{-S}^{(\pm)} = \pm\sqrt{1 \mp \frac{\chi}{\sqrt{1+\chi^2}}}. \quad (17)$$

Here, $\gamma = 2(\hbar S)^2/(I_z\Delta)$ and $\chi = \gamma J/S$. As is noted in equation (16), the ground state $E_{J-}$ switches to higher $J$ with increasing $\gamma$. The value of $\gamma$ at which the ground state changes from $E_{J-1,-}$ to $E_{J,-}$ is determined by $E_{J-1,-}(\gamma_J) = E_{J,-}(\gamma_J)$, which results in [24]

$$\gamma_J^{-2} = \left[1 - \frac{1}{(2S)^2}\right]\left[1 - \frac{(2J-1)^2}{(2S)^2}\right]. \quad (18)$$

Note that the ground state is shifted from $E_{0,-}$ to $E_{1,-}$ at $\gamma = \gamma_1$, from $E_{1,-}$ to $E_{2,-}$ at $\gamma = \gamma_2$, and so on. Taking $S = 10$ as an example, the critical value of $\gamma_J$ changes slowly and increases abruptly around $J = 8$ (Tab. 1).

## 4 Effect of the acoustic wave

We consider the spin dynamics generated by the acoustic wave. In order to deal with such a problem, we project the Hamiltonian (14) onto the two states basis $\{|\Phi_{J,+}^{(0)}\rangle, |\Phi_{J,-}^{(0)}\rangle\}$ with the coefficients in equation (17). Introducing a new pseudospin $\hat{\sigma}_i'$ by substituting $|\Phi_{J,+}^{(0)}\rangle$ and $|\Phi_{J,-}^{(0)}\rangle$ for $|S\rangle$ and $|-S\rangle$ in equation (8), respectively, one obtains a new spin Hamiltonian without a constant

$$\bar{\mathcal{H}}_J^{(\mathrm{lat})} = \frac{1}{2}\sqrt{1+\chi^2}\left[1 - \frac{2qp\chi}{1+\chi^2}\sin(pt')\right]\sigma_z' + \frac{qp\sin(pt')}{\sqrt{1+\chi^2}}\sigma_x', \quad (19)$$

where $x$ has been treated as a parameter, allowing $t - kx/\omega$ to be replaced by $t$. Also, we have made the replacement $\tilde{\mathcal{H}}_{\mathrm{eff},L}^{(\mathrm{lat})} \to \bar{\mathcal{H}}_J^{(\mathrm{lat})}\Delta$ and introduced the dimensionless parameters

$$t' = t\left(\frac{\Delta}{\hbar}\right), \quad p = \frac{\hbar\omega}{\Delta}, \quad q = \frac{\omega_R}{\omega}. \quad (20)$$

The time-dependent Schrödinger equation is:

$$i\frac{\partial}{\partial t'}\left|\Psi_J^{(\mathrm{lat})}\right\rangle = \bar{\mathcal{H}}_J^{(\mathrm{lat})}\left|\Psi_J^{(\mathrm{lat})}\right\rangle. \quad (21)$$

We expand $|\Psi_J^{(\mathrm{lat})}\rangle$ in the two states of the two-level system ( $|\Phi_{J,\pm}^{(0)}\rangle$ ) according to:

$$\left|\Psi_J^{(\mathrm{lat})}\right\rangle = a_+\left|\Phi_{J,+}^{(0)}\right\rangle + a_-\left|\Phi_{J,-}^{(0)}\right\rangle. \quad (22)$$

Inserting this equation into equation (21) yields:

$$i\dot{a}_\pm = \mp\frac{1}{2}E_0\left[1 - \epsilon\sin(pt')\right]a_\pm + V_0\sin(pt')a_\mp, \quad (23)$$

where the dot indicates differentiation with respect to the time $t'$ and

$$E_0 = \sqrt{1+\chi^2}, \quad \epsilon = \frac{2qp\chi}{1+\chi^2}, \quad V_0 = \frac{qp}{\sqrt{1+\chi^2}}. \quad (24)$$

Let us introduce new amplitudes, $\alpha_\pm(t')$, according to

$$a_\pm(t') = \exp\left[\pm\frac{i}{2}E_0\left(t' + \frac{\epsilon}{p}\cos(pt')\right)\right]\alpha_\pm(t'). \quad (25)$$

Then, we obtain from equation (23):

$$i\dot{\alpha}_\pm = V_0\sin(pt')\exp\left[\mp iE_0\left(t' + \frac{\epsilon}{p}\cos(pt')\right)\right]\alpha_\mp. \quad (26)$$

In order to study such a problem, we need to know the initial conditions based on possible experimental situations. In fact, the sample is initially in the $|\Phi_{J,+}^{(0)}\rangle$ state, in which there is no acoustic wave, after which the acoustic power is applied to the sample at frequency $\omega \simeq (\Delta/\hbar)E_0$ and maintained throughout the whole process. In this case, the initial conditions become $a_+(0) = 1$ and $a_-(0) = 0$, which corresponds to $\alpha_+(0) = 1$ and $\dot{\alpha}_+(0) = 0$ from equations (25) and (26). The set of equations (26) is difficult to solve in general. However, writing it in the form

$$i\dot{\alpha}_\pm = -\frac{iV_0}{2}\left[e^{i(p\mp E_0)t'} - e^{-i(p\pm E_0)t'}\right] \times \exp\left[\mp i\frac{\epsilon E_0}{p}\cos(pt')\right]\alpha_\mp, \quad (27)$$

we notice that the $\exp[\pm i(p-E_0)t']$ term varies slowly with $t'$ close to resonance ($p \simeq E_0$), while the $\exp[\pm i(p+E_0)t']$ term varies rapidly with time. Assuming that the effect of the rapidly varying terms is small, we discard these terms and keep only the slowly varying term[2]: $\exp[\pm i(p-E_0)t]$. The result is

$$i\dot{\alpha}_{\pm} \simeq \mp\frac{iV_0}{2}e^{\pm i(p-E_0)t'}\exp\left[\mp i\frac{\epsilon E_0}{p}\cos(pt')\right]\alpha_{\mp}. \quad (28)$$

After a little bit of manipulation, we obtain the second-order differential equation for $\alpha_+$:

$$\ddot{\alpha}_+ - i\left(a + 2\varepsilon\sin\tau\right)\dot{\alpha}_+ + b^2\alpha_+ = 0, \quad (29)$$

where the dot denotes differentiation with respect to the time $\tau$ ($= pt'$), and $a = 1 - E_0/p$, $\varepsilon = \epsilon E_0/(2p)$, and $b = V_0/(2p)$. Note that equation (29) is simplified when the system is on resonance ($a = 0$ ($p = E_0$) and $\epsilon = 0$):

$$\ddot{\alpha}_+ + b^2\alpha_+ = 0, \quad (30)$$

where $b$ is the Rabi frequency. For $\varepsilon \neq 0$, we need to solve equation (29) numerically. Noting that $\varepsilon \ll 1$ in the range which we are interested in, it is meaningful to employ perturbation theory to obtain approximate solutions to the problem (29). A perturbative solution is constructed by local analysis about $\varepsilon$ as a power series expansion:

$$\alpha_+(\tau) = \sum_{n=0}^{\infty}\varepsilon^n\alpha_{+n}(\tau), \quad (31)$$

where $\alpha_{+0}(0) = 1$, $\dot{\alpha}_{+0}(0) = 0$, and $\alpha_{+n}(0) = 0$, $\dot{\alpha}_{+n}(0) = 0$ ($n \geq 1$). To obtain the first term in this series, we set $\varepsilon = 0$ in equation (29) and solve

$$\ddot{\alpha}_{+0} - ia\dot{\alpha}_{+0} + b^2\alpha_{+0} = 0. \quad (32)$$

This expression is easy to handle and we obtain the solution which satisfies the initial conditions given by

$$\alpha_{+0}(\tau) = e^{\frac{i}{2}a\tau}\left[\cos\left(\frac{\Omega\tau}{2}\right) - i\frac{a}{\Omega}\sin\left(\frac{\Omega\tau}{2}\right)\right], \quad (33)$$

where $\Omega = \sqrt{a^2+4b^2}$. The $n$th-order problem ($n \geq 1$) is obtained by substituting equation (31) into equation (29) and setting the coefficient of $\varepsilon^n$ ($n \geq 1$) equal to 0. The result is

$$\ddot{\alpha}_{+n} - ia\dot{\alpha}_{+n} + b^2\alpha_{+n} = 2i\dot{\alpha}_{+n-1}\sin\tau, \quad (34)$$

with $\alpha_{+n}(0) = \dot{\alpha}_{+n}(0) = 0$. Note that perturbation theory has replaced the intractable differential equation (29) with a sequence of inhomogeneous equations (34). To solve equation (34) at $n = 1$, we rewrite the inhomogeneous term, which results in

$$\frac{i}{4}\Omega\left[1-\left(\frac{a}{\Omega}\right)^2\right]e^{\frac{i}{2}a\tau}\left[e^{\frac{i}{2}(\Omega+2)\tau} - e^{\frac{i}{2}(-\Omega+2)\tau} - e^{\frac{i}{2}(\Omega-2)\tau} + e^{\frac{i}{2}(-\Omega-2)\tau}\right]. \quad (35)$$

[2] This procedure is called the rotating wave approximation which is discussed in reference [27].

In comparison to equations (32) and (33), the secular terms, whose amplitude grows with $\tau$, occur only if $\Omega = 1$. Since the amplitude of the system is not bounded in this situation, the appearance of secular terms signals the invalidity of a perturbation expansion for large $\tau$. In this instance, we first consider the perturbation method for $\Omega \neq 1$. Then, the first-order perturbative solution to equation (29) is

$$\alpha_{+1}(\tau) = \alpha_{+1,h}(\tau) + \alpha_{+1,p}(\tau), \quad (36)$$

where

$$\alpha_{+1,h}(\tau) = i\left(\frac{a^2-\Omega^2}{1-\Omega^2}\right)e^{\frac{i}{2}a\tau}\cos\frac{\Omega\tau}{2}, \quad (37)$$

$$\alpha_{+1,p}(\tau) = \frac{i}{2}\Omega\left[1-\left(\frac{a}{\Omega}\right)^2\right]e^{\frac{i}{2}a\tau} \times\left\{\frac{\cos\left[\left(1-\frac{\Omega}{2}\right)\tau\right]}{1-\Omega} - \frac{\cos\left[\left(1+\frac{\Omega}{2}\right)\tau\right]}{1+\Omega}\right\}. \quad (38)$$

Here, $h$ and $p$ denote the homogeneous and the particular solution, respectively. Similarly, we can find the first-order perturbative solution for $\Omega = 1$ given by:

$$\alpha^{(0)}_{+1}(\tau) = \alpha^{(0)}_{+1,h}(\tau) + \alpha^{(0)}_{+1,p}(\tau), \quad (39)$$

where

$$\alpha^{(0)}_{+1,h}(\tau) = \frac{i}{4}\left(1-a^2\right)e^{\frac{i}{2}a\tau}\cos\left(\frac{\tau}{2}\right), \quad (40)$$

$$\alpha^{(0)}_{+1,p}(\tau) = -\frac{i}{4}\left(1-a^2\right)e^{\frac{i}{2}a\tau} \times\left[\cos\left(\frac{3\tau}{2}\right) + 2\tau\sin\left(\frac{\tau}{2}\right)\right]. \quad (41)$$

For fixed $\tau$, the error between $\alpha^{(0)}_{+0}(\tau)$ and $\alpha^{(0)}_{+0}(\tau) + \varepsilon\alpha^{(0)}_{+1}(\tau)$ is at most of order $\varepsilon^2$ as $\varepsilon \to 0+$. This result emerges if we consider large values of $\tau$ – specifically, values of $\tau$ of order $1/\varepsilon$ or larger as $\varepsilon \to 0+$. For such large values of $\tau$, the secular term in $\alpha^{(0)}_{+1}(\tau)$ grows with $\tau$, which suggests the invalidity of perturbation expansions for large $\tau$.

Assuming that the spin was initially in the state $|\Phi^{(0)}_{J,+}\rangle$ and the acoustic wave is delivered to the sample at $t > 0$, the probability of finding the spin in the state $|\Phi^{(0)}_{J,+}\rangle$ becomes, from equations (4) and (15),

$$P_+(t') = \left|\left\langle\Phi^{(0)}_{J,+}\middle|\Psi\right\rangle\right|^2 = |a_+(t')\left[\cos\varphi - i\frac{\chi}{\sqrt{1+\chi^2}}\sin\varphi\right] - \frac{ia_-(t')}{\sqrt{1+\chi^2}}\sin\varphi|^2, \quad (42)$$

where $\varphi = q\cos(pt')$.

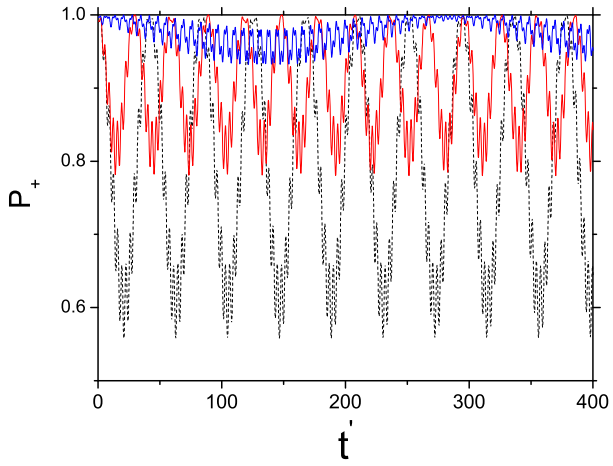


**Fig. 1.** Time dependence ($t' = t\Delta/\hbar$) of the probability ($P_+$) of finding the spin in the state $|\Phi^{(0)}_{J,+}\rangle$ from equation (29) at $x = 0$, $S = 10$, $p = 0.9$, and $q = 0.1$. Black dashed line: $J = 2$ and $\gamma = 1.03$ ($\varepsilon \simeq 0.0202$). Red solid line: $J = 4$ and $\gamma = 1.12$ ($\varepsilon \simeq 0.0409$). Blue solid line: $J = 8$ and $\gamma = 1.90$ ($\varepsilon \simeq 0.0835$).

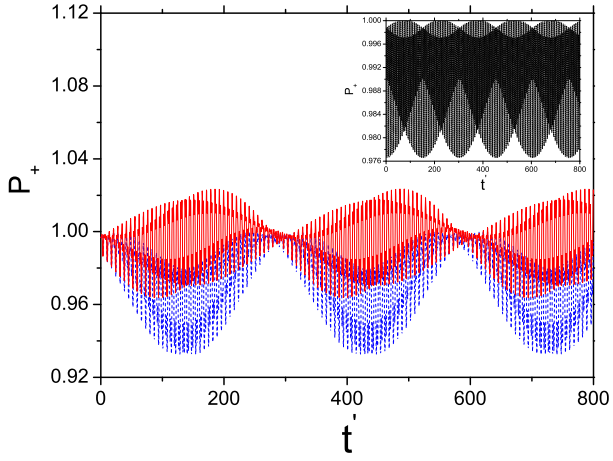


**Fig. 2.** $P_+$ vs. $t'$ at $x = 0$, $S = 10$, $p = 0.9$, $q = 0.1$, $J = 8$, and $\gamma = 1.9$. Blue dashed line: numerical result from equation (29). Red solid line: the first-order perturbative result. Inset: the zeroth-order perturbative result for comparison.

Numerical calculations show that there are several frequencies involved (Fig. 1). What is interesting is the existence of the beat structure of $P_+$ at $J = 8$ and $\gamma = 1.9$, which corresponds to $\varepsilon \simeq 0.0835$. In order to discuss the structure of the beat, it is desirable to obtain the analytic expression of $P_+$ by using the perturbative result of $a_\pm$ discussed previously. Hence, we first need to obtain the zeroth- and the first-order perturbative results for $|a_\pm(t)|^2$, $a_+(t)a^*_-(t)$. Plugging equations (31), (33), and (36) into (42), we get the approximate probability given by:

$$P_+(t') \simeq P^{(0)}(t') + \varepsilon P^{(1)}(t'), \tag{43}$$

where

$$P^{(i)}(t') = A^{(i)}_c \cos^2\varphi + A^{(i)}_s \sin^2\varphi + A^{(i)}_{cs} \cos\varphi \sin\varphi, \tag{44}$$

with $A^{(i)}_k = A^{(i)}_k(p\Omega, pt')$, $i = 0, 1$, and $k = c, s, cs$ (Appendix). As is shown in Figure 1, there are several frequencies involved. In order to find the optimal beat condition amongst them, we make use of equations (43), (A.1), and (A.2). Simple analysis shows that the beat structure is expected to be more pronounced at the frequency $\Omega \simeq 1$, which gives the relation

$$p^{(\Omega\simeq 1)} \simeq \frac{(1+\chi^2)^{3/2}}{q^2}\left(1 - \sqrt{1 - \frac{q^2}{1+\chi^2}}\right). \tag{45}$$

Taking $\gamma = 1.9$, $J = 8$, $S = 10$, and $q = 0.1$ as an example, we obtain $p \simeq 0.91$ and thereby find the optimal beat structure (Fig. 2).

Next, we consider the magnetic moment of the system. Noting that $L_z$ in this formalism describes the mechanical rotation of the molecular magnet as a whole, not the orbital states of the electrons, the magnetic moment of a loosely fastened molecular magnet is generated by the expectation value of the $z$ projection of the spin given by

$$\langle\Psi|\hat{S}_z|\Psi\rangle = S\left(\left|a_+(t')C^{(+)}_S + a_-(t')C^{(-)}_S\right|^2 - 1\right), \tag{46}$$

where the magnetic moment becomes $-g\mu_B\langle\Psi|\hat{S}_z|\Psi\rangle$. Here, $g$ is the spin gyromagnetic factor and $\mu_B$ the Bohr magneton. Plugging equations (4) and (22) into equation (46), we obtain

$$\langle\hat{S}_z\rangle/S = \left(|a_+(t')|^2 - |a_-(t')|^2\right)\frac{\chi}{\sqrt{1+\chi^2}} + \frac{1}{\sqrt{1+\chi^2}}\left[a_+(t')a^*_-(t') + a^*_+(t')a_-(t')\right], \tag{47}$$

where $\langle\Psi|\hat{S}_z|\Psi\rangle \equiv \langle\hat{S}_z\rangle$. Equations (28) and (29) have been solved numerically. Figure 3 illustrates the situation at zero and nonzero $J$ for a given value of $p$ and $q$. For several values of $\gamma$ in Table 1, the period of $\langle\hat{S}_z\rangle$ is about 47 at $J = 0$, 42 at $J = 2$, 30 at $J = 4$, and 300 at $J = 8$. The first three results agree with the frequencies $p\Omega$ ($= \sqrt{(p - E_0)^2 + V_0^2}$). However, the most striking feature of the magnetization dynamics observed in simulation is the largest beat generated at $J = 8$ and $\gamma = 1.9$ in Figure 3. In order to understand such a feature, we need to make use of the perturbative results (33) and (36). Then, we have

$$\langle\hat{s}_z(t')\rangle \simeq \langle\hat{s}_z(pt')\rangle_0 + \varepsilon\langle\hat{s}_z(pt')\rangle_1, \tag{48}$$

where $\langle\hat{s}_z\rangle = \langle\hat{S}_z\rangle/S$ and

$$\langle\hat{s}_z(t)\rangle_0 = \frac{1}{2\sqrt{1+\chi^2}\Omega^2}\left\{2a^2\chi + 8b^2\chi\cos(\Omega t) + 4ab\sin t + 2(a+\Omega)b\sin[(\Omega-1)t] - 2(a-\Omega)b\sin[(\Omega+1)t]\right\}, \tag{49}$$

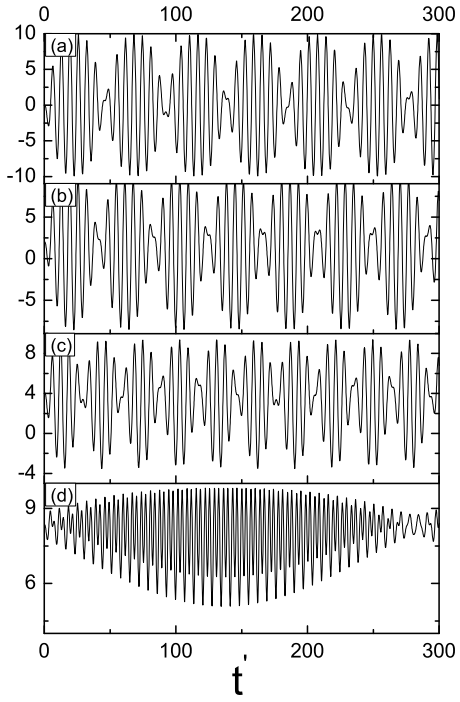


**Fig. 3.** The plot of $\langle \hat{S}_z \rangle$ as a function of $t'$ at $x = 0$, $S = 10$, $p = 0.9$, and $q = 0.1$. Here, (a) $J = 0$ and $\gamma = 0$, (b) $J = 2$ and $\gamma = 1.03$, (c) $J = 4$, and $\gamma = 1.12$, and (d) $J = 8$, and $\gamma = 1.9$.

$$\begin{aligned}\langle \hat{s}_z(t)\rangle_1 = \frac{1}{\sqrt{1+\chi^2}\Omega^2(\Omega^2-1)}\{&-2ab(1+a)\\ &+2(a-1)ab\cos(2t)\\ &+2b(a-4b^2-a\Omega^2)\cos(\Omega t)\\ &+2ab\Omega(a+\Omega)\cos[(\Omega-1)t]\\ &+(1-a)b(1+\Omega)(a+\Omega)\cos[(\Omega-2)t]\\ &+2ab\Omega(\Omega-a)\cos[(\Omega+1)t]\\ &+(a-1)b(a-\Omega)(\Omega-1)\cos[(\Omega+2)t]\\ &+8ab^2\chi\sin t-8ab^2\chi\Omega\sin(\Omega t)\\ &+4ab^2\chi(1+\Omega)\sin[(\Omega-1)t]\\ &+4ab^2\chi(\Omega-1)\sin[(\Omega+1)t]\}. \end{aligned} \quad (50)$$

As is shown in Figure 4, the first-order perturbative result is sufficiently good to give a numerical result. In this respect, it is meaningful to discuss the optimal conditions for generating the larger beat structures. Even though there are several frequencies involved in equations (49) and (50), such a condition is produced by the frequency $\Omega \simeq 1$, which corresponds to relation (45). Large beats are also expected to occur at $\Omega \simeq 2$, which leads to the relation

$$1/p^{(\Omega\simeq 2)} \simeq \frac{1}{\sqrt{1+\chi^2}}\left(1+\sqrt{4-\frac{q^2}{1+\chi^2}}\right). \quad (51)$$

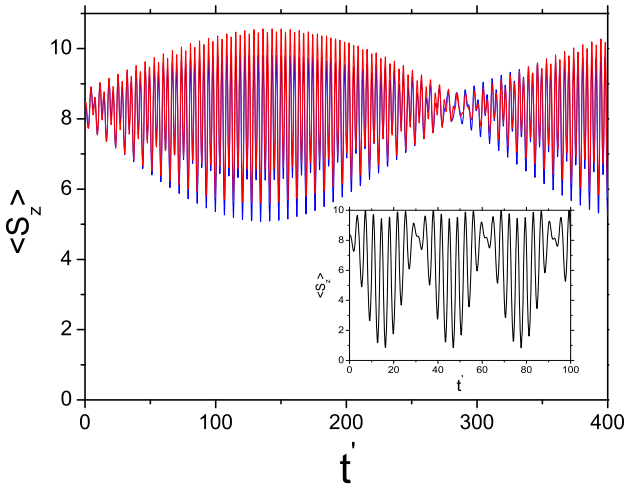


**Fig. 4.** The $t'$ dependence of $\langle \hat{S}_z \rangle$ at $x = 0$, $S = 10$, $p = 0.9$, $q = 0.1$, $J = 8$, and $\gamma = 1.9$. Blue solid line: numerical result from equations (29) and (46). Red solid line: the first-order perturbative result from equation (48). Note that the beat and the oscillatory behavior are almost the same in both cases. Inset: numerical result at $p = 1.638(=0.9E_0)$ with $E_0 \simeq 1.819$ for comparison.

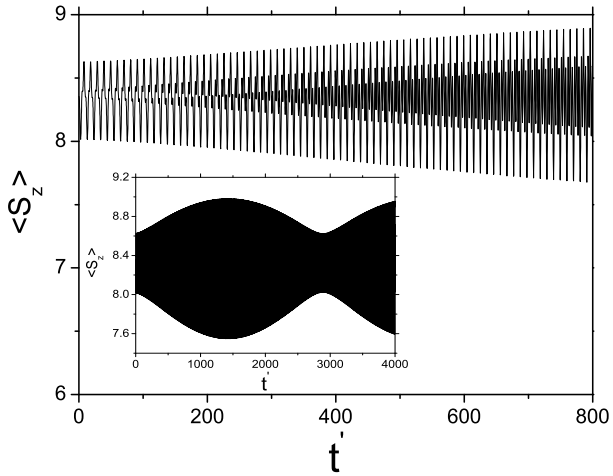


**Fig. 5.** $\langle \hat{S}_z \rangle$ vs. $t'$ at $x = 0$, $S = 10$, $p = 0.606$, $q = 0.1$, $J = 8$, and $\gamma = 1.9$. Inset: oscillation for a wider range of $t'$. Note that the beat period tends to be larger at $\Omega \simeq 2$ than $\Omega \simeq 1$ (Fig. 4).

Taking $q = 0.1$, $J = 8$ and $\gamma = 1.9$ as an example and putting them into equation (51), we have $p \simeq 0.606$. Hence, for $p \simeq 0.606$ the period of the beat is approximately given by 3290 $[\simeq 2\pi/(2p - p\Omega)]$ (Fig. 5). This is simply understood by plotting $p$ as a function of $\chi$. As is shown in Figure 6, $p^{(\Omega\simeq 2)}$ becomes smaller than $p^{(\Omega\simeq 1)}$, which results in $p^{(\Omega\simeq 1)}/p^{(\Omega\simeq 2)} \simeq 1.5$ in the range of $\chi$ under consideration. Thus, the ratio of the beat periods, $T^{(\Omega\simeq 2)}/T^{(\Omega\simeq 1)}$, becomes much larger.

Before concluding, it is meaningful to discuss the decoherence by phonons and spin-bath, which might be

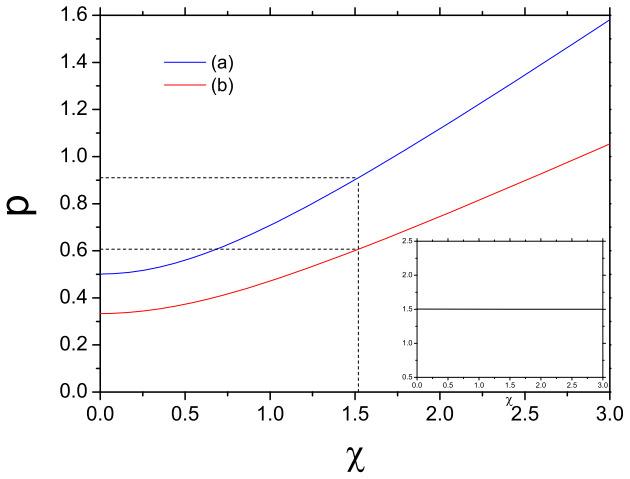


**Fig. 6.** $p$ vs. $\chi$ for the large beat at $\Omega \simeq 1$ (a), and $\Omega \simeq 2$ (b). Note that $p \simeq 0.91$ (a) and 0.605 (b) at $\chi = 1.52$, which comes from the system with $\gamma = 1.9$, $J = 8$, and $S = 10$. Inset: $p^{(\Omega\simeq 1)}/p^{(\Omega\simeq 2)}$ as a function of $\chi$. Note that the approximate value of $p^{(\Omega\simeq 1)}/p^{(\Omega\simeq 2)}$ becomes 1.5.

important for the observability of the effects. The lower bound on the decoherence due to spin-lattice interactions can be estimated as the spin-phonon relaxation rate [20] $\Gamma_{\rm ph}$. Taking $\omega \sim \Delta/\hbar \sim 100$ GHz, $u_0 \sim 1$ nm, $\rho \sim 1$ g/cm$^3$, $S = 10$, and $c_t \sim 10^5$ cm/s for typical molecular magnets, one obtains $\Gamma_{\rm ph} \sim 16.8$ KHz $\ll \Omega_B \sim 91.9$ GHz, where $\Omega_B = p\Omega(\Delta/\hbar)$. Also, noting that the typical hyperfine field $H_{\rm hf}$ is of the order of 0.1 Oe, the relaxation rate produced by the spin-bath becomes $\Gamma_s \simeq (g\mu_B/\hbar)H_{\rm hf} \sim 1$ MHz. Hence, the decoherence rate generated by phonons and environmental spins are much lower than the beat frequencies involved, and it is therefore feasible to observe quantum oscillations in the molecular magnets which we have considered.

## 5 Conclusion

We have demonstrated that, in the presence of sound waves, the period of the quantum oscillation due to spin tunneling in free SMMs can be strongly influenced by the moment of inertia of the SMM and its total angular momentum. Employing the rotating wave approximation and perturbation theory, we have derived the approximate form of the expectation value of the $Z$ projection of the spin and compared it to the numerical result. Using the first-order perturbative formula, we have obtained the optimal condition for generating large beat structures, and found that two conditions can generate macroscopic quantum beats in the magnetization of a free SMM. These features are expected to be observable in experiments.

This research was supported by the Basic Science Research Program through the National Research Foundation of Korea (NRF), funded by the Ministry of Education, Science and Technology (2012-0002696).

## Appendix: Parameters in equation (44)

The zeroth-order terms are

$$
\begin{aligned}
A_c^{(0)}(\Omega,t) &= \frac{1}{2\Omega^2}\left[a^2+\Omega^2+4b^2\cos(\Omega t)\right],\\
A_s^{(0)}(\Omega,t) &= \frac{1}{2(1+\chi^2)\Omega^2}\{4b^2+\chi^2(a^2+\Omega^2)\\
&\quad +4b[a\chi\sin t-\cos(\Omega t)(b-bx^2+a\chi\sin t)\\
&\quad +\chi\Omega\cos t\sin(\Omega t)]\},\\
A_{cs}^{(0)}(\Omega,t) &= \frac{b}{\Omega^2\sqrt{1+\chi^2}}\Bigg\{-\Omega\sin(\Omega t)\sin t\\
&\quad +2a\cos t\sin^2\left(\frac{\Omega t}{2}\right)\Bigg\},
\end{aligned}
\tag{A.1}
$$

and the first-order ones are

$$
\begin{aligned}
A_c^{(1)}(\Omega,t) &= \frac{4ab^2}{\Omega^2(\Omega^2-1)}\{[1-\cos(\Omega t)]\sin t\\
&\quad -\Omega(1-\cos t)\sin(\Omega t)\},\\
A_s^{(1)}(\Omega,t) &= \frac{2b}{(1+\chi^2)\Omega^2(\Omega^2-1)}\Bigg\{-a(1+a)\chi\\
&\quad +(1-a)\chi\cos(2t)[-a+(a+\Omega^2)\cos(\Omega t)]\\
&\quad +2ab(-1+\chi^2)\sin t\\
&\quad +\cos(\Omega t)\left[\chi(a-4b^2-a\Omega^2+2a\Omega^2\cos t)\right.\\
&\quad \left.+2ab(1-\chi^2)\sin t\right]\\
&\quad +2\Omega\sin\left(\frac{t}{2}\right)\Bigg[\left(1+a^2\right)\chi\cos\left(\frac{t}{2}\right)\\
&\quad +\left(1-a^2\right)\chi\cos\left(\frac{3t}{2}\right)\\
&\quad +2ab(1-\chi^2)\sin\left(\frac{t}{2}\right)\Bigg]\sin(\Omega t)\Bigg\},\\
A_{cs}^{(1)}(\Omega,t) &= \frac{2b}{\Omega^2(\Omega^2-1)\sqrt{1+\chi^2}}\{2\left[-a\Omega^2\right.\\
&\quad \left.+(-1+a)(a+\Omega^2)\cos t\right]\cos(\Omega t)\sin t\\
&\quad +2\cos t\left[(1-a)a\sin t\right.\\
&\quad \left.+\Omega(a^2+\cos t-a^2\cos t)\sin(\Omega t)\right]\}.
\end{aligned}
\tag{A.2}
$$

## References

1. *Quantum Tunneling of Magnetization-QTM '94*, edited by L. Gunther, B. Barbara (Kluwer Academic, Dordrecht/Boston/London, 1995)
2. E.M. Chudnovsky, J. Tejada, *Lectures on Magnetism* (Rinton Press, Paramus, NJ, 2006)
3. D. Gatteschi, R. Sessoli, J. Villain, *Molecular Nanomagnets* (Oxford University Press, Oxford, 2006)

4. J.R. Friedman, M.P. Sarachik, J. Tejada, R. Ziolo, Phys. Rev. Lett. **76**, 3830 (1996)
5. L. Thomas, F. Lionti, R. Ballou, D. Gatteschi, R. Sessoli, B. Barbara, Nature **383**, 145 (1996)
6. C. Sangregorio, T. Ohm, C. Paulsen, R. Sessoli, D. Gatteschi, Phys. Rev. Lett. **78**, 4645 (1997)
7. R. Caciuffo, G. Amoretti, A. Murani, R. Sessoli, A. Caneschi, D. Gatteschi, Phys. Rev. Lett. **81**, 4744 (1998)
8. W. Wernsdorfer, T. Ohm, C. Sangregorio, R. Sessoli, D. Mailly, C. Paulsen, Phys. Rev. Lett. **82**, 3903 (1999)
9. A. Garg, Europhys. Lett. **22**, 205 (1993)
10. W. Wernsdorfer, R. Sessoli, Science **284**, 133 (1999)
11. S. Bertaina, S. Gambarelli, T. Mitra, B. Tsukerblat, A. Müller, B. Barbara, Nature **453**, 203 (2008)
12. G.-H. Kim, T.-S. Kim, Phys. Rev. Lett. **92**, 137203 (2004)
13. C. Romeike, M.R. Wegewijs, W. Hofstetter, H. Schoeller, Phys. Rev. Lett. **96**, 196601 (2006)
14. H.B. Heersche, Z. de Groot, J.A. Folk, H.S.J. van der Zant, C. Romeike, M.R. Wegewijs, L. Zobbi, D. Barreca, E. Tondello, A. Cornia, Phys. Rev. Lett. **96**, 206801 (2006)
15. M.N. Leuenberger, E.R. Mucciolo, Phys. Rev. Lett. **97**, 126601 (2006)
16. M.-H. Jo, J.E. Grose, K. Baheti, M.M. Deshmukh, J.J. Sokol, E.M. Rumberger, D.N. Hendrickson, J.R. Long, H. Park, D.C. Ralph, Nano Lett. **6**, 2014 (2006)
17. M. Misiorny, J. Barnaś, Phys. Rev. B **75**, 134425 (2007)
18. L. Bogani, W. Wernsdorfer, Nat. Mater. **7**, 179 (2008)
19. S. Barraza-Lopez, K. Park, V. García-Suárez, J. Ferrer, Phys. Rev. Lett. **102**, 246801 (2009)
20. E.M. Chudnovsky, D.A. Garanin, R. Schilling, Phys. Rev. B **72**, 094426 (2005)
21. C. Calero, E.M. Chudnovsky, Phys. Rev. Lett. **99**, 047201 (2007)
22. G.-H. Kim, E.M. Chudnovsky, Phys. Rev. B **79**, 134404 (2009)
23. G.-H. Kim, Eur. Phys. J. B **81**, 451 (2011)
24. E.M. Chudnovsky, D.A. Garanin, Phys. Rev. B **81**, 214423 (2010)
25. L.D. Landau, E.M. Lifshitz, *Theory of Elasticity* (Pergamon Press, New York, 1959)
26. E.M. Chudnovsky, D.A. Garanin, R. Schilling, Phys. Rev. B **72**, 094426 (2005)
27. K. Gottfried, T.-M. Yan, *Quantum Mechanics: Fundamentals* (Springer-Verlag, Berlin, 2003)